

PRACTICAL MANUAL FOR FLUORESCENCE MICROSCOPY TECHNIQUES

Sohail Ahmed
Sudhaharan Thankiah
Radek Machán
Martin Hof
Andrew H. A. Clayton
Graham Wright
Jean-Baptiste Sibarita
Thomas Korte
Andreas Herrmann

4 chapter

Fluorescence Lifetime Imaging Microscopy by TCSPC (TD-FLIM)

Thomas Korte¹ and Andreas Herrmann²
*Humboldt-University Berlin, Institute of Biology,
Group of Molecular Biophysics, Berlin, Germany*
Contact details: ¹thomas.korte@rz.hu-berlin.de,
²andreas.herrmann@rz.hu-berlin.de

Index

1. Principle and Theory.....	3
Principle of TCSPC	3
Characterization of Lipid Organization and Membrane Structures of Model Systems and Biological Membranes by FLIM	4
Measurement of FRET via FLIM	5
2. Instrumentation.....	6
3. Method	6
Characterization of the Lateral Distribution of the Transmembrane Domain of the Fusion Protein of Influenza Virus in CHO-K1 Cells	6
Materials Required	7
Sample Preparation.....	7
4. Data Acquisition	7
5. Data Analysis.....	8
6. Results and Data Verification	10
7. Limitations and Trouble Shooting	10
8. Conclusions and Applications.....	10
Acknowledgments	11
References and Further Reading	12
Appendix.....	14
(A) Step-by-step guide for the measurement of CFP/YFP FLIM-FRET using an Olympus FV1000 CLSM with PicoQuant LSM FLIM and FCS upgrade kit	14
(B) Video links for FLIM data acquisition.....	17
(C) SPT64 links for FLIM data analysis.....	17
(D) Tipps/Tricks	17

1. Principle and Theory

Fluorescence Lifetime Imaging is a single molecule technique which uses the detection of fluorescence lifetime instead of fluorescence intensities to obtain information on the environment of the fluorophore or the interaction of molecules labelled with a donor-acceptor pair via FRET. There are two ways for the acquisition of lifetime data, measurements in the frequency domain (see chapter FD-FLIM by Andrew H.A. Clayton) or in the time domain as introduced here (TD-FLIM). Both techniques use different equipment and have individual advantages. The frequency method is mainly used on wide field fluorescence microscopes. It can be directly performed with fast imaging detectors like CCD cameras with additional time-gating equipment and it often requires a shorter time for data acquisition. Measurements in the time domain are single point measurements

combined with a scanning method using for instance Confocal Laser Scanning Microscopes (CLSM). This intuitive method provides a higher sensitivity since single photon counting detectors are used, a better time resolution can be obtained and it provides more options for the analysis of multi-exponential fluorescence decays.

Principle of TCSPC

After absorption of light, a fluorophore molecule remains for a certain time (usually several nanoseconds) in the excited state before returning to the ground state, either by emitting a photon or by non-radiative energy transfer. The transition from the excited state to the ground state is a statistical process and therefore the emission of fluorescence photons follows an exponential decay law. The average time between excitation and the emission of fluorescence light for a large number of cycles

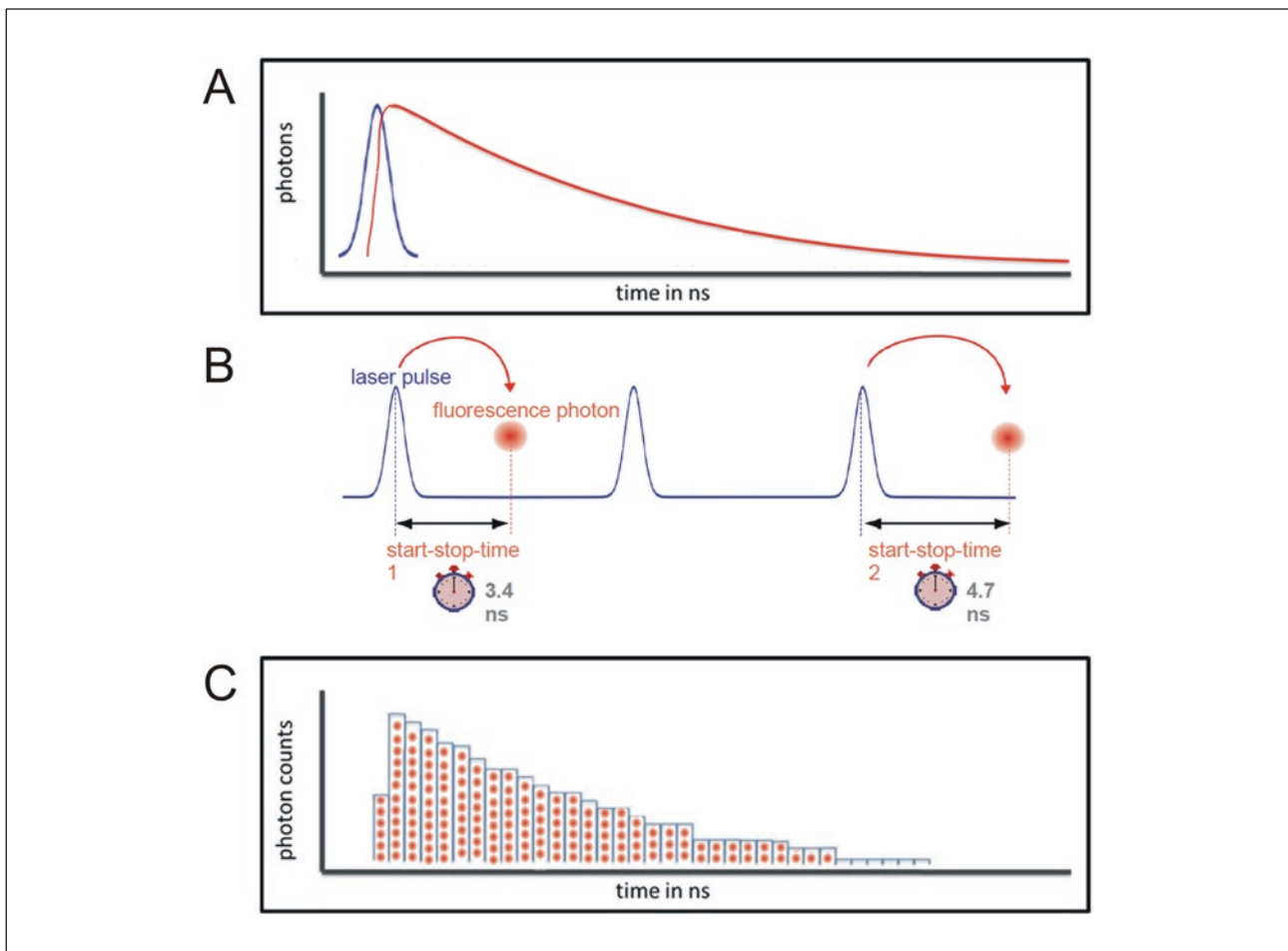


Figure 1 Principle of TCSPC. **A** Excitation of a large number of fluorophore molecules with a short flash of light results in an exponential decay of emitted photons. **B** Instead of detecting the complete time dependent emission profile from one excitation – emission cycle, periodic excitation by a pulsed laser is used and a large number of single photons are recorded, at maximum one per excitation pulse. The difference between the start (trigger of laser) and the stop (signal from the detector) is measured by electronics that acts like a stop watch. **C** The arrival times are grouped into bins (“channels”) with picosecond time resolution and a histogram of their distribution is build up.

is called the fluorescence lifetime of a fluorescent molecule. The lifetime is an intrinsic property of a fluorophore based on the stability of the excited state. However, since it depends on its local environment it can be used to monitor changes in the immediate surrounding or to detect conformational changes within molecules as well as molecular interactions with other molecules via FRET (see Figure 1).

Lifetime measurements in the time domain require recording of lifetimes of a large number of molecules. After excitation with a short flash of light, commonly a laser pulse, the time dependent intensity profile of emitted light is detected. Since it is physically impossible to detect the required number of photons from one excitation – emission cycle, periodic excitation by a pulsed laser is used and a large number of single photons are recorded. This method is called Time-Correlated Single Photon Counting (TCSPC). After excitation by a short laser pulse the precise time of the detection of single photon is registered, the reference for the timing is the corresponding excitation pulse. The difference between the start (trigger pulse of laser) and the stop (arrival of electronic pulse from the detector) is measured by electronics that acts like a stop watch. With periodic excitation and the detection of a large number of individual photons, arrival times are grouped into bins (often called time channels) with picosecond time resolution and a histogram of their distribution is build up. By adjusting laser power and repetition rate, the probability of registering more than one photon per cycle is kept low to avoid the pile-up effect. The typical result is a TCSPC histogram with an exponential drop of counts at increasing times. This histogram reflects the fluorescence decay and is analyzed by fitting to

exponential decay function(s) to extract the fluorescence lifetime(s) and the amplitude(s).

Characterization of Lipid Organization and Membrane Structures of Model Systems and Biological Membranes by FLIM

As mentioned above, the fluorescence lifetime of a fluorophore depends on its local environment, which can be influenced by factors like temperature, pH and interactions with other fluorescent and non-fluorescent molecules. The fluorescence lifetime is thereby more sensitive to these influences than other spectral parameters, like the steady state fluorescence emission intensity or wavelength, and since it is a single molecule method it is less dependent on measurement artefacts like varying (local) concentrations and bleaching. One application of TD-FLIM measurements in our lab is the characterization of the lateral organization of artificial and biological membranes using fluorescently labelled phospholipids.

For many biological processes domains enriched in cholesterol, phospholipids and/or (glyco)sphingolipids with long saturated acyl and alkyl chains - so called “rafts” - have been discussed to play an important role for instance as reactions platforms or sites of protein interaction. However, presumably due to their small size and their short lifetime detailed knowledge about them, especially in live cells under physiological conditions, is elusive. It has been shown, that distinct liquid-ordered (lo) and -disordered (ld) domains can be induced in model membranes by the variation of the lipid composition. Giant Unilamellar Vesicles (GUVs) have been established as valuable tool to visualize lipid domain formation using various

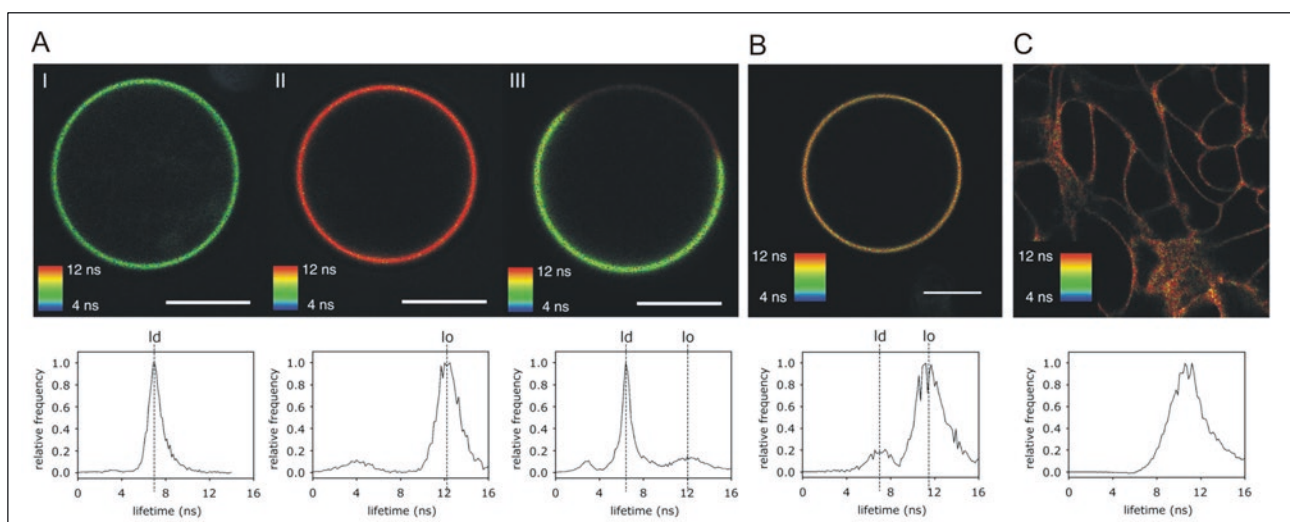


Figure 2 Fluorescence lifetimes of C6-NBD-PC in different membranes. **A** C6-NBD-PC in GUV prepared from DOPC (I, pure ld phase), DOPC/SSM/Chol=1/1/8 (II; pure lo phase) and DOPC/SSM/Chol=1/1/1 (III; ld and lo phase) at 25 °C. (Scale bars 10 μ m). **B** GUV prepared from POPC/PSM/Chol=4/2/4 (no visible domains). **C** HepG2-cells. Top row: average lifetime (see scale), Bottom row: respective lifetime histograms. (maximum normalized to 1) From [23].

lipid-like fluorophors, which enrich either in the l_o or in the l_d domain (see Figure 2).

We have employed phospholipid analogues labelled with the fluorophore NBD to characterize lipid domains in GUVs and the plasma membrane of mammalian cells by TD-FLIM^{[1],[2]}. C6-NBD-phosphatidylcholine incorporates into both phases, the fluorescence decay of the NBD fluorophore is characterized by a short and long lifetime. The latter was found to be strongly dependent on the lipid environment: a large difference in the fluorescence lifetime was found for lipid mixtures forming pure l_o or l_d vesicles, we measured fluorescence lifetimes of about 12 ns (l_o) and 7 ns (l_d), respectively. The same localization-dependent lifetimes were obtained for GUVs forming microscopically visible lipid domains (Figure 2A). Moreover, even at a lipid composition showing no visible lateral lipid segregation (POPC/PSM/Chol=4/2/4) the lifetime diagram indicated the coexistence of submicroscopic domains in GUV (Figure 2B), which is in agreement with a previous study based on FRET measurements on LUV^{[3],[4]}. NBD-labelled phospholipid analogues can easily be incorporated into the plasma membrane of mammalian cells, they have been previously established as marker for phospholipid transport. HepG2- cells were labeled with C6-NBD-PC and the distribution of fluorescence lifetimes was studied. For plasma membrane and intracellular membrane compartments different average lifetimes were observed, reflecting the differences in membrane composition. No microscopically visible domains could be resolved when analyzing the plasma membranes of HepG2 cells labelled with C6-NBD-PC, however, a broad distribution of the fluorescence lifetime around 10-11ns was observed (see Figure 2C) suggesting the coexistence of various submicroscopic domains. These results show, the TD-FLIM studies are a valuable tool for the investigation of lipid organization and membrane structures, but also protein localization and protein-lipid-interaction in model systems and biological membranes.

Measurement of FRET via FLIM

The principle and theory of Förster Resonance Energy Transfer (FRET) is given elsewhere in great detail^[13], here only a short summary: In essence, FRET is the transfer of energy from an excited donor molecule to an acceptor fluorophore in close vicinity by non-radiative dipole-dipole coupling. This results in quenching of the donor indicated by its lower fluorescence intensity and shorter fluorescence lifetime as well as increasing of the acceptor fluorescence intensity. The efficiency of the transfer depends mainly on (a) the spectral overlap of donor emission and acceptor excitation, (b) the distance of donor and acceptor molecule ($<10\text{nm}$) and (c) the orientation of the fluo-

rophore dipoles. Commonly, FRET can be detected by imaging of the acceptor fluorescence after donor excitation (sensitized emission) or by comparing the donor emission in the presence and the absence of the acceptor. The latter is usually achieved by photobleaching of the acceptor (see chapter AP-FRET). However, these methods are based on the intensity and therefore can be influenced by fluorophore concentration (e.g. the expression level for genetically encoded fluorescent proteins), background fluorescence, spectral cross-talk, and bleaching of the donor as well as the acceptor.

Another method to determine the presence of FRET is measurement of the donor excited state lifetime (FLIM-FRET). For measurements in the time domain (td-FLIM) the quenching of the donor fluorescence lifetime detected by the TCSPC method is analyzed. Because in the presence of FRET the donor molecule has an additional non-radiative pathway to return to the ground state, its fluorescence lifetime is shortened, resulting in a faster drop of the fluorescence decay. Since the fluorescence lifetime is independent of the fluorophore concentration, FLIM-FRET enables quantitative measurements and straightforward comparison of different samples (e.g. cells) with varying fluorophore amount. It is notable, that due to the very steep distance dependence of the FRET efficiency, especially in cells with typical protein concentrations in the micro molar range, the average distance between molecules is too large for false positive FRET, even at high molecular concentrations.

The fluorescence decay curve is analyzed by fitting it to a mono or multi exponential function and the parameters fluorescence lifetime and fractional amplitude can be extracted. As a unique feature, FLIM-FRET allows to resolve subpopulations if only a fraction of donor-labeled molecules is bound in a complex. The prerequisite is a mono-exponentially decaying donor fluorophore. In case of FRET, the decay curve exhibits a bi-exponential behavior consisting of a short lifetime corresponding to the FRET quenched donor molecules and a longer lifetime of unquenched donors. Based on the amplitudes of these two lifetime components, the fraction of free and associated molecules can be determined. This procedure can be applied to every image pixel and the differences in the lifetime distribution can be visualized by a color-coded FLIM image. This enables to visualize e.g. the presence or absence of FRET as well as the localization of the subpopulations along the sample.

between GPI-CFP as raft marker and the YFP-tagged transmembrane domain (TMD) of HA to characterize the mechanism of the lateral organization of the viral fusion protein in the plasma membrane of eukaryotic cells, in particular its recruitment to raft domains. This recruitment has been associated with specific properties of the transmembrane domain (TMD) and the cytoplasmic tail of HA^[9-11]. GPI stands for Glycosylphosphatidylinositol which is a lipid anchored structure. Its localization to raft domains has been demonstrated previously^{[12],[13]}.

Materials Required

Chinese hamster ovary cells (CHO-K1, American Type Culture Collection), for which the presence of cholesterol-sensitive lipid nanodomains and their dimension in the plasma membrane have been described^[12]. FBS, Antibiotics (penicillin and streptomycin), Trypsin, plasmids for GPI and TMD-HA tagged with CFP and YFP, respectively, DMEM media and transfection reagent (Lipofectamine 2000). 35mm glass-bottom-dishes (MatTek, Ashland, MA), T75 flasks and pipettes and other cell culture supplies.

Sample Preparation

1. CHO-K1 cells (ATCC) are maintained in T75 flasks in DMEM with 10%FBS and 1% Penicillin-Streptomycin at 37°C and 5% CO₂.
2. Cells were detached from the flask using 1,5 ml trypsin-EDTA by incubating at 37°C for 5 min.
3. Cells were seeded in 35mm glass-bottom-dishes and grown to ~80% confluence, transfection was carried out using Lipofectamine 2000 following the manufacturer's protocol (Invitrogen).
4. 20-24 h post transfection cells are washed, analyzed for expression of the fluorescent proteins and FLIM-FRET measurements are carried out in DMEM without phenol red.

In general, the following protein expressions would be ideal to provide sample and additional controls:

- a) Co-expression of x-donor and y-acceptor as experimental model where x and y are the proteins/molecules of interest
- b) Expression of x-donor alone (or even better co-expression of x-donor and non-tagged y) as negative control
- c) Co-expression of x-donor and y-acceptor where interaction is blocked or inactivated
- d) Tandem-fusion of donor and acceptor to one protein or sample with both proteins x-donor and y-acceptor expressed and cross-linked as positive control

In our case x-donor corresponds to the raft marker GPI-CFP and y-acceptor to TMD-HA-YFP. We are investigating the FRET caused by co-localization

of GPI-CFP and TMD-HA-YFP in raft domains, as control with an abandoned interaction (c) we are using cells depleted of cholesterol since this treatment has been shown to result in the disruption of rafts^[14]. As positive control (d) GPI-CFP and GPI-YFP were co-expressed, both should be incorporated into raft domains.

4. Data Acquisition

We are using an Olympus FV1000 confocal microscope equipped with a PicoQuant LSM upgrade kit for FLIM / FCS and the Software SymphoTime for acquisition and analysis of fluorescence lifetime data. A step-by-step guide for the acquisition of the data required for FLIM-FRET measurements is given in the Appendix. The PicoQuant LSM upgrade kit is available for CLSMs of all major manufacturers, with the help of the guide it should be easy to perform the measurements on suitable instrumentation of other suppliers.

The following data sets have to be acquired for the data analysis and the evaluation of the results:

1. Confocal Images of CFP and YFP expression in the sequential mode to monitor the expression of the individual proteins. Note: While the signal in Channel 2 shows the expression of YFP, the signal in Channel 1 reflects only CFP molecules not affected by FRET.
2. Confocal "Intensity" FRET image of the YFP fluorescence (excitation with 458nm) Channel 1 shows the CFP fluorescence intensity without FRET, channel 2 the YFP intensity due to FRET but also spill-over of CFP, acceptor emission due to direct excitation at 458 nm and eventually background-fluorescence. Therefore additional measurements like FLIM-FRET or acceptor photobleaching are necessary to obtain conclusive results.
3. FLIM image of CFP fluorescence (excitation with pulsed 440nm diode) recorded on the FLIM computer.
4. Measurement of the Internal response function (IRF) The overall timing precision of a complete TCSPC system is characterized by its Instrument Response Function (IRF). For an ideal system with an infinitely sharp excitation pulse and infinitely accurate detectors and electronics, the IRF should be infinitely narrow. Due to the properties of light source, detector and electronics, the IRF is broadened. Thus, to precisely analyze decay curves with short lifetimes the IRF has to be determined for the method of "n-Exponential Deconvolution" (see "Data analysis" below).

The best way to measure the IRF is to use a solution of a fluorophore with similar fluorescence properties as the sample but with a very short lifetime, which can be induced by a quencher at saturating concentration (for instance KJ).

If such a fluorophore is not available, one can alternatively record the scattering of the excitation light. In that case a narrow-band filter for the wavelength of the excitation light is placed in front of the detector. Since the IRF of some detectors is dependent on the wavelength, measurement at the excitation wavelength might not be useful for numerical reconvolution. The solution is to acquire the IRF at the emission wavelength, or at least spectrally closer to the fluorescence emission.

5. Data Analysis

In SymphoTime select regions of interest (ROI) of the images either by hand or using the magic wand tool. In our case, the plasma membrane of an individual cell is selected. First, all measured photons of the ROI are combined into a global histogram. This global decay curve is used to obtain the fitting parameters, which are afterwards used for the pixel by pixel fit and the generation of the fluorescence lifetime image (see Figure 4).

The SymPhoTime software allows to analyze the data either by “n-Exponential Tailfit” or by “n-Exponential Reconvolution”. Tail fitting can only be used when the fitted lifetimes are significantly longer than the IRF. It is not sufficient for a detailed analysis of the individual components of a multi-exponential decay. Therefore, for reconvolution the correspond-

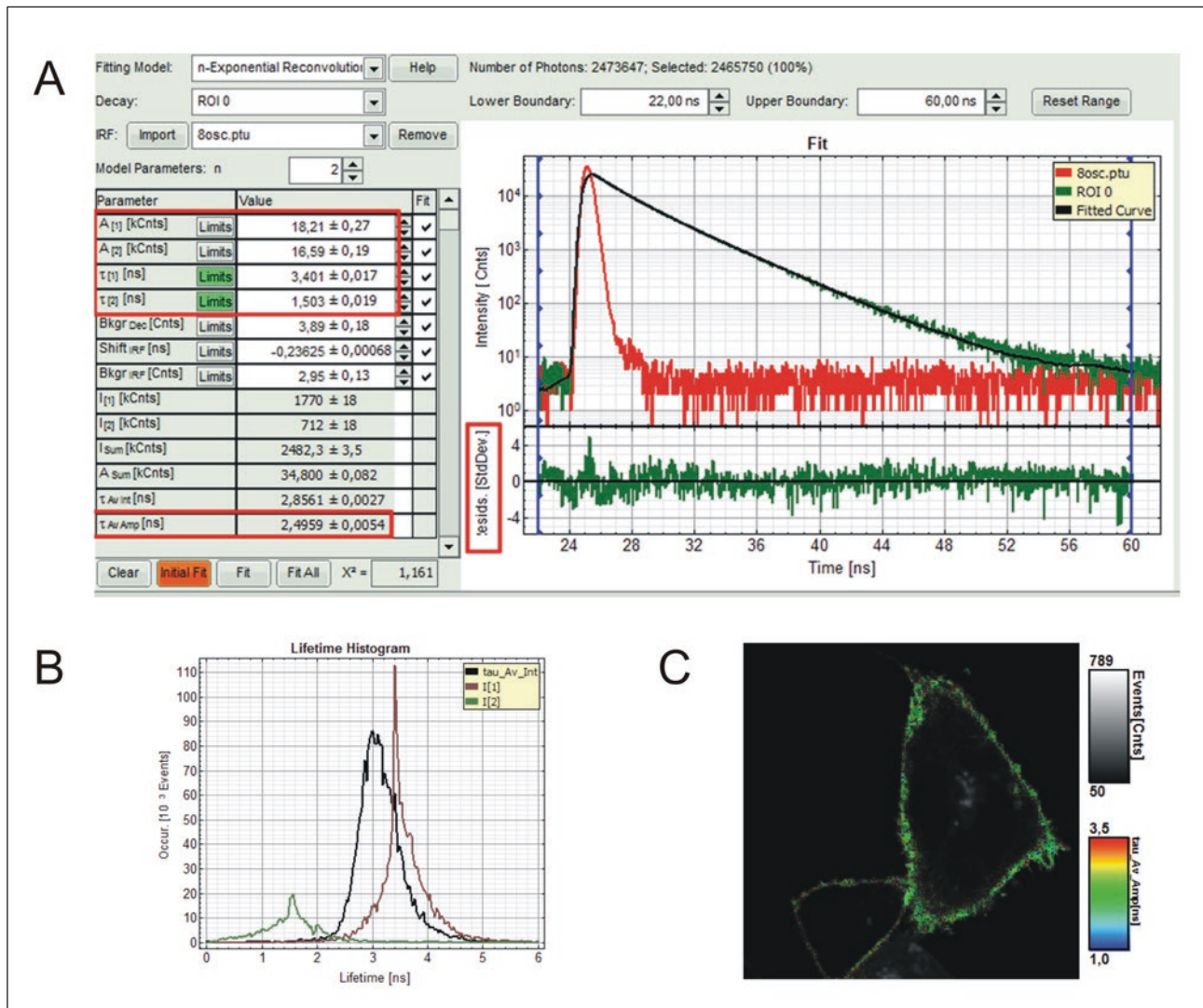


Figure 4 Analysis of fluorescence lifetime data using SymphoTime 64. **A** Decay curve for a ROI (green), imported IRF (red), biexponential curve fit (black). Important parameters are highlighted with red boxes. **B** Lifetime histogram with distribution of lifetimes. **C** Color-coded fluorescence lifetime image.

ing IRF has to be imported. Alternatively, the IRF is reconstructed in the software by directly evaluating the onset of the fluorescence decay. Afterwards, the decay curve is analyzed by fitting it using a nonlinear least squares iterative procedure to a mono or multi-exponential function. First the control sample (GPI-CFP only) is processed. Our constructs contain ECFP as donor, which has been shown to express an intrinsic biexponential fluorescence decay with lifetimes of about 1.3 and 3.8 ns^{[15],[16]}. Therefore, the fitting procedure is started with two exponential components, the quality of the fit is judged by the distribution of the residuals and the goodness of fit parameter (χ^2). The χ^2 value should be close to 1, the fitted curve should overlay well with the decay curve, the calculated fitting values must be reasonable and the residuals representing the deviation of the fit from the measured decay curve should be small and randomly distributed. An exemplary fit with the highlighted parameters is shown in Figure 4A. If the fit is not satisfying, especially if a tendency can be seen in the distribution of the residuals, an additional exponential should be added, all parameters have to be cleared and the fit has to be repeated. An additional exponential is for instance needed if different populations of the donor occur (FRET and non-FRET, different local environment) or to correct for deviations in the beginning of the curve due to a not perfectly fitting IRF.

Parameters obtained from the SymphoTime software are the lifetime τ_i and amplitude A_i of the individual exponential component. The quantification of the individual exponential terms is complicated by the biexponential decay of CFP. Therefore, for every ROI the amplitude-weighted average lifetime of CFP is calculated using the following equation^[17]:

$$\tau_{Av Amp} = \frac{\sum_{k=0}^{n-1} A[k] \tau[k]}{A_{Sum}}$$

SymPhoTime uses two ways of calculating the average lifetime ($\tau_{AV int}$ and $\tau_{AV amp}$) differing in the way the single decay times are weighted, $\tau_{AV amp}$ is proportional to the steady state intensity and therefore applicable for the calculation of the FRET efficiency based on the donor lifetimes.

The FRET efficiency (E) is defined as the proportion of the donor molecules that have transferred excitation state energy to the acceptor molecules. It is calculated for each ROI using the equation

$$E = \left[1 - \frac{\tau_{Av Amp}}{\tau_D} \right]$$

where τ_{DA} is the amplitude-weighted average lifetime of the donor in the presence of the acceptor and τ_D is the one of 10 control cells (donor GPI-CFP expressed alone). To generate lifetime images (for instance in order to compare lifetimes in different compartments), afterwards each pixel of the selection is analyzed based on the parameters obtained with a maximum likelihood estimation and a color coded FLIM image and a lifetime distribution histogram are generated (see Figure 4B and C). A sufficient number of cells have to be analyzed, the mean and standard error have to be calculated to compare the different samples and measured differences have to be verified by statistical tests and appropriate controls.

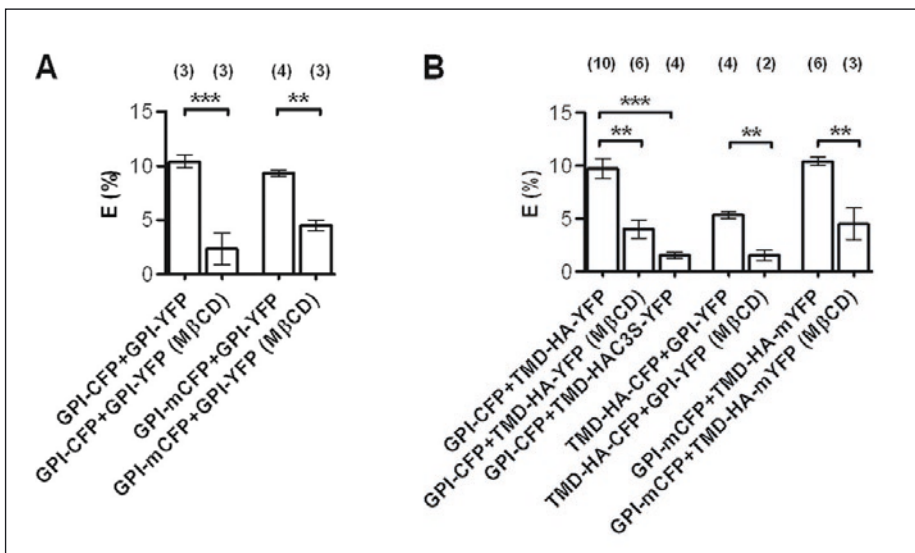


Figure 5 Interaction between GPI and TMD-HA constructs measured by FLIM- FRET. FRET efficiency between raft markers (A), between raft marker and different TMD-HA variants (B), MβCD, after pretreatment with MβCD to disrupt liquid ordered domains in the plasma membrane. Above the bars, n refers to the number of independent experiments is given. Each experiment is based on 10 cells. Data represent the mean ± S.E. **, p < 0.0001, ** p < 0.005. Experiments were carried out at 25 °C. (from Scolari et al., 2009)

6. Results and Data Verification

We have used this method to characterize the lateral distribution of the TMD of HA in CHO-K1 cells and purified plasma membranes^[8]. Co-expression of the raft-marker GPI-CFP with TMD-HA-YFP led to a significant shortening of donor lifetime in comparison to cells expressing GPI-CFP only. This could be attributed to FRET indicating sorting of TMD-HA-YFP into raft domains in the plasma membrane, FRET efficiency was calculated to about 10% (Figure 5). Cholesterol depletion using methyl- β -cyclodextrin (M β CD) has been shown to result in the disruption of ordered domains in biological membranes^[14]. This treatment of the plasma membrane resulted in a decrease of FRET between GPI-CFP and TMD-HA-YFP, while CFP lifetime in cells expressing only the donor GPI-CFP was not affected. As positive control, co-expression of GPI-CFP and GPI-YFP, which both should be enriched in raft domains, resulted also in a shortening of CFP lifetime and a FRET efficiency of about 10%, which was significantly reduced by M β CD treatment.

7. Limitations and Trouble Shooting

While genetic labeling with fluorescent proteins has become a valuable tool for live-cell imaging and the detection of protein-protein interaction by FRET, there are also several limitations. Due to the large size of the fluorescent proteins, which are 4.2nm long with a 2.4 nm barre^{[18],[19]}, a large part of the usable FRET is occupied resulting in a maximum FRET efficiency of about 40%. If two proteins are labeled on opposite sites or in case the dipole moments of donor and acceptor are not properly aligned, FRET might not be measurable even if the proteins of interest are bound to each other. Also, tagging of proteins with these large markers might change the folding, transport or localization of the proteins which are investigated. Some of the fluorescent proteins (also ECFP) have the tendency to form homodimers by themselves, which can reduce the fluorescence lifetime and therefore could lead to false-positive results^[20]. Therefore CFP variants shown to be monomeric should be used^{[13],[16]}, also the ratio donor : acceptor should be kept low in order to prevent dimerization of the donor and to improve the signal-to-noise ratio. To obtain the full content of information allowing to quantify the FRET results, it is crucial to use a donor fluorophore with a mono-exponential decay. FLIM-FRET measurements are based on a statistical analysis of a sufficient number of photons, therefore image acquisition is in most cases longer than for Intensity-FRET or FLIM-FRET in the frequency domain, for dynamic processes this might require fixation of the sample.

8. Conclusions and Applications

Measurement of FRET by FLIM is a highly sensitive method that can be used to detect protein-protein interactions in vivo. Since only the donor fluorescence lifetime is detected and analyzed, it is not dependent on variations in the protein expression level, a problem often occurring in cellular systems – especially if more than one protein is expressed by transfection. Compared to intensity-based FRET measurements, FLIM-FRET leads to quantitative results and, if the donor fluorescence can be described by a mono-exponential decay, allows to identify sub-populations that undergo FRET. Another advantage of measurements in the time domain (td-FLIM) is that this is a single molecule method and therefore performed on a very low illumination level, which prevents photo damage and bleaching. Also, since this is a point scanning method, illumination can be restricted to the area of interest and time for data acquisition can be reduced by selecting a smaller area or scanning resolution.

Finally, the whole decay curve is recorded and therefore more sophisticated analysis can be performed, also it is possible to detect two (or more) fluorescence channels at the same time and to use the information from the second channel to gate or correlate the data analyzed.

Over the last years, the td-FLIM has been established as valuable tool not only to measure protein-protein interaction but also protein localization in membranes and protein-ligand binding. The table below shows a selection of recent publications using td-FLIM and FLIM-FRET measurements for in vivo studies.

Applications	Method / FRET-Pair	Ref.
Receptor phosphorylation / dephosphorylation	td-FLIM (FLIM-FRET)	[21], [22]
Receptor localization (IgE-FcεRI) in microdomains	td-FLIM	[23]
Characterization of membrane properties in model and biological membranes	td-FLIM	[24], [1], [25], [2], [26], [27]
Phospholipid traffic in cells	td-FLIM	[28], [29]
Influence of ABC transporters on membrane composition	td-FLIM	[30]
NAD(P)H to visualize pathogen-host interactions	td-FLIM	[31]
In Vivo imaging of specific probes to cancer biomarkers	td-FLIM	[32]
Interaction site of cellular actin with the plasma membrane	GFP and RFP	[33]
Interaction of chemokine receptor CXCR4 and protein kinase C	GFP and RFP	[34]
Membrane localization of viral proteins	CFP and YFP Cer and YFP	[8], [11], [35]
Interaction of poxvirus proteins with kinesin	GFP and DsRed	[36]
Interaction of proteins in yeast	Cer and YFP	[37]
Complexes of t- and v-SNARE in fungi	Cer and Ven	[38]
Interaction of plasma membrane proteins in maize	CFP and YFP	[39]
Interaction of serotonin receptors in different cell lines	GFP and mCherry	[40]
Cell division multi-protein complex in Streptomyces	GFP and mCherry	[41]
Interaction of Golgi tethering factors and small GTPases	GFP and mRFP	[42]
Interactions of proteins related to Alzheimer's disease	GFP and mRFP	[43]
Receptor-Ligand interaction in endocytosis and trafficking	YFP and Cy3.5 GFP and mRFP	[44] [45]
Characterization of membrane fusion	lipid markers	[46]

Acknowledgments

We are thankful to Dr. Sandra Orthaus (PicoQuant GmbH, Germany) for helpful comments and editing of this manuscript.

References and Further Reading

- [1] Stöckl, M., et al., Detection of lipid domains in model and cell membranes by fluorescence lifetime imaging microscopy of fluorescent lipid analogues. *J Biol Chem*, 2008. 283(45): p. 30828-37.
- [2] Stöckl, M. and A. Herrmann, Detection of lipid domains in model and cell membranes by fluorescence lifetime imaging microscopy. *Biochim Biophys Acta*, 2010. 1798(7): p. 1444-56.
- [3] de Almeida, R.F., A. Fedorov, and M. Prieto, Sphingomyelin/phosphatidylcholine/cholesterol phase diagram: boundaries and composition of lipid rafts. *Biophys J*, 2003. 85(4): p. 2406-16.
- [4] de Almeida, R.F., et al., Lipid rafts have different sizes depending on membrane composition: a time-resolved fluorescence resonance energy transfer study. *J Mol Biol*, 2005. 346(4): p. 1109-20.
- [5] Scheiffele, P., et al., Influenza viruses select ordered lipid domains during budding from the plasma membrane. *J Biol Chem*, 1999. 274(4): p. 2038-44.
- [6] Takeda, M., et al., Influenza virus hemagglutinin concentrates in lipid raft microdomains for efficient viral fusion. *Proc Natl Acad Sci U S A*, 2003. 100(25): p. 14610-7.
- [7] Wagner, A.J., S. Loew, and S. May, Influence of Monolayer-Monolayer Coupling on the Phase Behavior of a Fluid Lipid Bilayer. *Biophys J*, 2007.
- [8] Scolari, S., et al., Lateral distribution of the transmembrane domain of influenza virus hemagglutinin revealed by time-resolved fluorescence imaging. *J Biol Chem*, 2009. 284(23): p. 15708-16.
- [9] Scheiffele, P., M.G. Roth, and K. Simons, Interaction of influenza virus haemagglutinin with sphingolipid-cholesterol membrane domains via its transmembrane domain. *Embo J*, 1997. 16(18): p. 5501-8.
- [10] Melkonian, K.A., et al., Role of lipid modifications in targeting proteins to detergent-resistant membrane rafts. Many raft proteins are acylated, while few are prenylated. *J Biol Chem*, 1999. 274(6): p. 3910-7.
- [11] Engel, S., et al., FLIM-FRET and FRAP reveal association of influenza virus haemagglutinin with membrane rafts. *Biochem J*, 2010. 425(3): p. 567-73.
- [12] Sharma, P., et al., Nanoscale organization of multiple GPI-anchored proteins in living cell membranes. *Cell*, 2004. 116(4): p. 577-89.
- [13] Zacharias, D.A., et al., Partitioning of lipid-modified monomeric GFPs into membrane microdomains of live cells. *Science*, 2002. 296(5569): p. 913-6.
- [14] Hao, M., S. Mukherjee, and F.R. Maxfield, Cholesterol depletion induces large scale domain segregation in living cell membranes. *Proc Natl Acad Sci U S A*, 2001. 98(23): p. 13072-7.
- [15] Tramier, M., et al., Picosecond-hetero-FRET microscopy to probe protein-protein interactions in live cells. *Biophys J*, 2002. 83(6): p. 3570-7.
- [16] Rizzo, M.A., et al., An improved cyan fluorescent protein variant useful for FRET. *Nat Biotechnol*, 2004. 22(4): p. 445-9.
- [17] Lackowicz, J.R., *Principles of Fluorescence Spectroscopy*. 2006, New York.: Springer Science+Business Media.
- [18] Ormo, M., et al., Crystal structure of the *Aequorea victoria* green fluorescent protein. *Science*, 1996. 273(5280): p. 1392-5.
- [19] Yang, F., L.G. Moss, and G.N. Phillips, Jr., The molecular structure of green fluorescent protein. *Nat Biotechnol*, 1996. 14(10): p. 1246-51.
- [20] Piston, D.W. and G.J. Kremers, Fluorescent protein FRET: the good, the bad and the ugly. *Trends Biochem Sci*, 2007. 32(9): p. 407-14.
- [21] Peltan, I.D., et al., Fluorescence lifetime imaging microscopy (FLIM) detects stimulus-dependent phosphorylation of the low density lipoprotein receptor-related protein (LRP) in primary neurons. *Biochem Biophys Res Commun*, 2006. 349(1): p. 24-30.
- [22] Treanor, B., et al., Microclusters of inhibitory killer immunoglobulin-like receptor signaling at natural killer cell immunological synapses. *J Cell Biol*, 2006. 174(1): p. 153-61.
- [23] Davey, A.M., et al., Membrane order and molecular dynamics associated with IgE receptor cross-linking in mast cells. *Biophys J*, 2007. 92(1): p. 343-55.
- [24] Margineanu, A., et al., Visualization of membrane rafts using a perylene monoimide derivative and fluorescence lifetime imaging. *Biophys J*, 2007. 93(8): p. 2877-91.
- [25] de Almeida, R.F., L.M. Loura, and M. Prieto, Membrane lipid domains and rafts: current applications of fluorescence lifetime spectroscopy and imaging. *Chem Phys Lipids*, 2009. 157(2): p. 61-77.
- [26] Bastos, A.E., et al., Applications of fluorescence lifetime spectroscopy and imaging to lipid domains in vivo. *Methods Enzymol*, 2012. 504: p. 57-81.
- [27] Sezgin, E., et al., Partitioning, diffusion, and ligand binding of raft lipid analogs in model and cellular plasma membranes. *Biochim Biophys Acta*, 2012. 1818(7): p. 1777-1784.
- [28] Wustner, D., Fluorescent sterols as tools in membrane biophysics and cell biology. *Chem Phys Lipids*, 2007. 146(1): p. 1-25.
- [29] Wustner, D., et al., Quantitative assessment of sterol traffic in living cells by dual labeling with dehydroergosterol and BODIPY-cholesterol. *Chem Phys Lipids*, 2011. 164(3): p. 221-35.

- [30] Zarubica, A., et al., Functional implications of the influence of ABCA1 on lipid microenvironment at the plasma membrane: a biophysical study. *FASEB J*, 2009. 23(6): p. 1775-85.
- [31] Szaszak, M., et al., Fluorescence lifetime imaging unravels *C. trachomatis* metabolism and its crosstalk with the host cell. *PLoS Pathog*, 2011. 7(7): p. e1002108.
- [32] Ardeshirpour, Y., et al., In vivo fluorescence lifetime imaging monitors binding of specific probes to cancer biomarkers. *PLoS One*, 2012. 7(2): p. e31881.
- [33] Konig, I., J.P. Schwarz, and K.I. Anderson, Fluorescence lifetime imaging: association of cortical actin with a PIP3-rich membrane compartment. *Eur J Cell Biol*, 2008. 87(8-9): p. 735-41.
- [34] Peter, M., et al., Multiphoton-FLIM quantification of the EGFP-mRFP1 FRET pair for localization of membrane receptor-kinase interactions. *Biophys J*, 2005. 88(2): p. 1224-37.
- [35] Thaa, B., et al., Intrinsic membrane association of the cytoplasmic tail of influenza virus M2 protein and lateral membrane sorting regulated by cholesterol binding and palmitoylation. *Biochem J*, 2011. 437(3): p. 389-97.
- [36] Jeshtadi, A., et al., Interaction of poxvirus intracellular mature virion proteins with the TPR domain of kinesin light chain in live infected cells revealed by two-photon-induced fluorescence resonance energy transfer fluorescence lifetime imaging microscopy. *J Virol*, 2010. 84(24): p. 12886-94.
- [37] Schreiber, G., et al., Unraveling interactions of cell cycle-regulating proteins Sic1 and B-type cyclins in living yeast cells: a FLIM-FRET approach. *FASEB J*, 2012. 26(2): p. 546-54.
- [38] Valkonen, M., et al., Spatially segregated SNARE protein interactions in living fungal cells. *J Biol Chem*, 2007. 282(31): p. 22775-85.
- [39] Zelazny, E., et al., FRET imaging in living maize cells reveals that plasma membrane aquaporins interact to regulate their subcellular localization. *Proc Natl Acad Sci U S A*, 2007. 104(30): p. 12359-64.
- [40] Fjorback, A.W., et al., Serotonin transporter oligomerization documented in RN46A cells and neurons by sensitized acceptor emission FRET and fluorescence lifetime imaging microscopy. *Biochem Biophys Res Commun*, 2009. 380(4): p. 724-8.
- [41] Willemsse, J., et al., Positive control of cell division: FtsZ is recruited by SsgB during sporulation of *Streptomyces*. *Genes Dev*, 2011. 25(1): p. 89-99.
- [42] Osterrieder, A., et al., Fluorescence lifetime imaging of interactions between Golgi tethering factors and small GTPases in plants. *Traffic*, 2009. 10(8): p. 1034-46.
- [43] Herl, L., et al., Mutations in amyloid precursor protein affect its interactions with presenilin/gamma-secretase. *Mol Cell Neurosci*, 2009. 41(2): p. 166-74.
- [44] Nievergall, E., et al., PTP1B regulates Eph receptor function and trafficking. *J Cell Biol*, 2010. 191(6): p. 1189-203.
- [45] Bu, W., et al., Cdc42 interaction with N-WASP and Toca-1 regulates membrane tubulation, vesicle formation and vesicle motility: implications for endocytosis. *PLoS One*, 2010. 5(8): p. e12153.
- [46] Dumas, F., et al., Spatial regulation of membrane fusion controlled by modification of phosphoinositides. *PLoS One*, 2010. 5(8): p. e12208.

Appendix

(A) Step-by-step guide for the measurement of CFP/YFP FLIM-FRET using an Olympus FV1000 CLSM with PicoQuant LSM FLIM and FCS upgrade kit

The Olympus Fluoview software on one computer (Imaging) is used to control the confocal microscope while the PicoQuant SymPhoTime software on a second computer (FLIM) is used for FLIM data acquisition and analysis. Both computers are connected by a network cable and the small tool SymPhoTime_RC can be used to remote-control the image acquisition of the SymPhoTime software from the Imaging computer.

1. Starting of the microscope and the software

Switch on the microscope, the appropriate lasers, the Imaging computer and the FLIM computer.

On the Imaging computer, start SymPhoTime_RC and Fluoview software. On the FLIM computer, start SymPhoTime and open a new workspace.

2. Selecting an objective, focussing the microscope and configuring the laser scanning and detection for confocal image acquisition.

Select 60x/1.35 Oil UPlanSApo objective and focus the sample using white light then search for cells having fluorescence tags using mercury lamp and focus them. Load the predefined settings for eCFP/eYFP. This will excite fusion proteins of CFP/YFP using the 458 nm and the 515 nm laser line as excitation source for confocal imaging, the primary dichroic mirror should be set to DM405-458/515/561/633 and the secondary dichroic mirror to SMD510. Activate the TD-channel to get an additional DIC image.

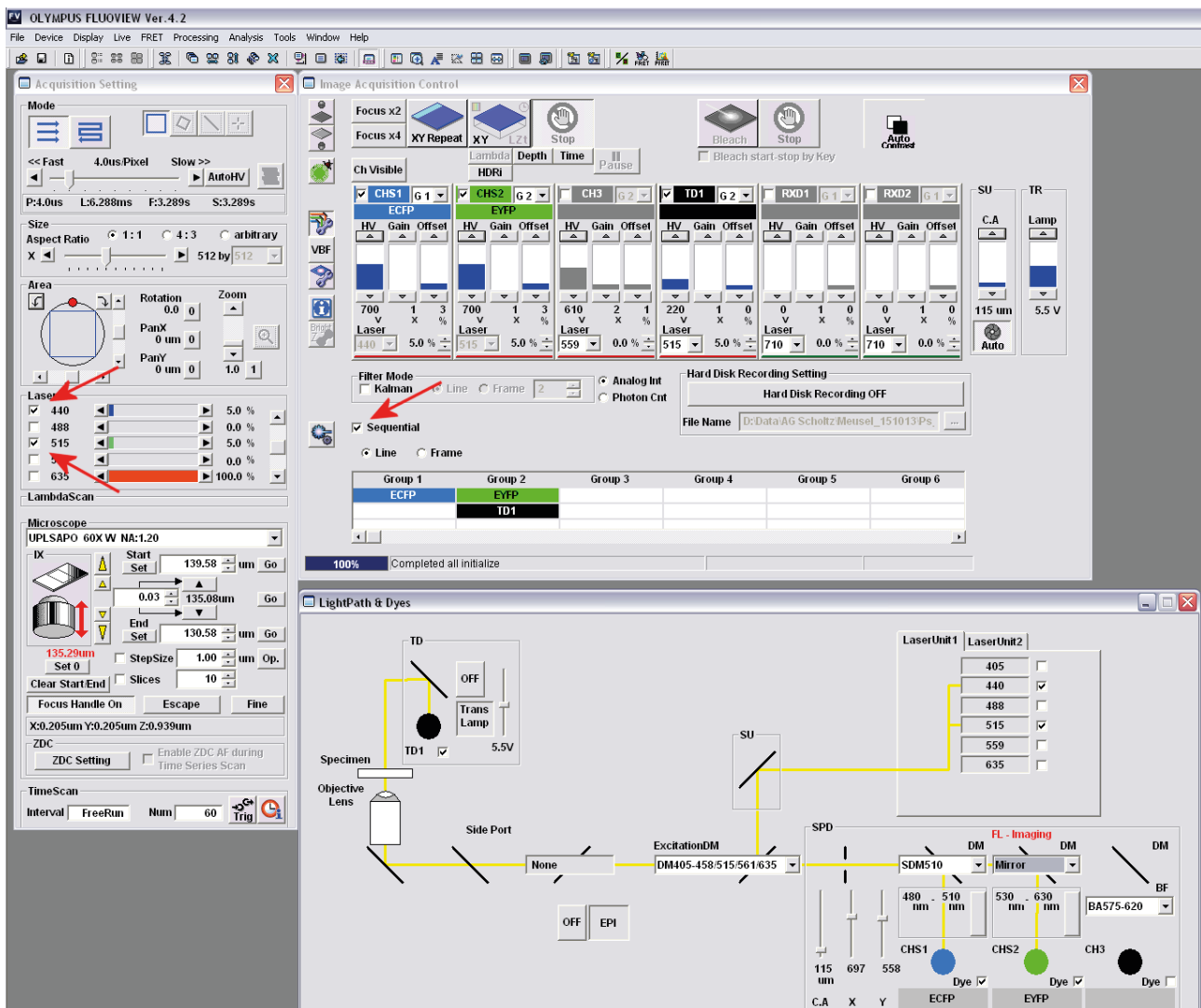


Figure A1 Settings of FV-1000 software for confocal imaging of CFP and YFP expression individually. Sequential scan with 458 nm and 515 nm laser lines.

3. Acquisition of confocal images

To Monitor the expression of the individual proteins, take an image in the sequential mode. Under those conditions CFP and YFP are excited and detected alternately. (Figure A1) Deactivate the 515nm excitation and the sequential mode and take an "Intensity" FRET image. (Figure A2) Channel 1 shows the CFP fluorescence intensity, channel 2 the YFP intensity due to FRET but also spill-over of CFP, acceptor emission due to direct excitation at 458 nm and eventually background-fluorescence. Therefore additional measurements like FLIM-FRET or acceptor photo-bleaching are necessary to obtain conclusive results.

4. Configuring the microscope and laser settings for FLIM imaging

For FLIM-FRET Imaging, only CFP is excited using a pulsed 440nm diode laser, images are recorded with the PicoQuant Detector Unit, in our case equipped with SPAD detectors and connected to the output port of the FV1000 scanner unit by fiber optics. Therefore all cw-lasers have to be deactivated and the light path has to be changed so the signal is routed to the output port. (see Figure A3)

The pulsed laser diodes have to be switched on and off either by hand or with additional hardware via the *FluoView* software like in our setup. Therefore all pulsed diode lasers are handled as 635nm laser independent of the wavelength

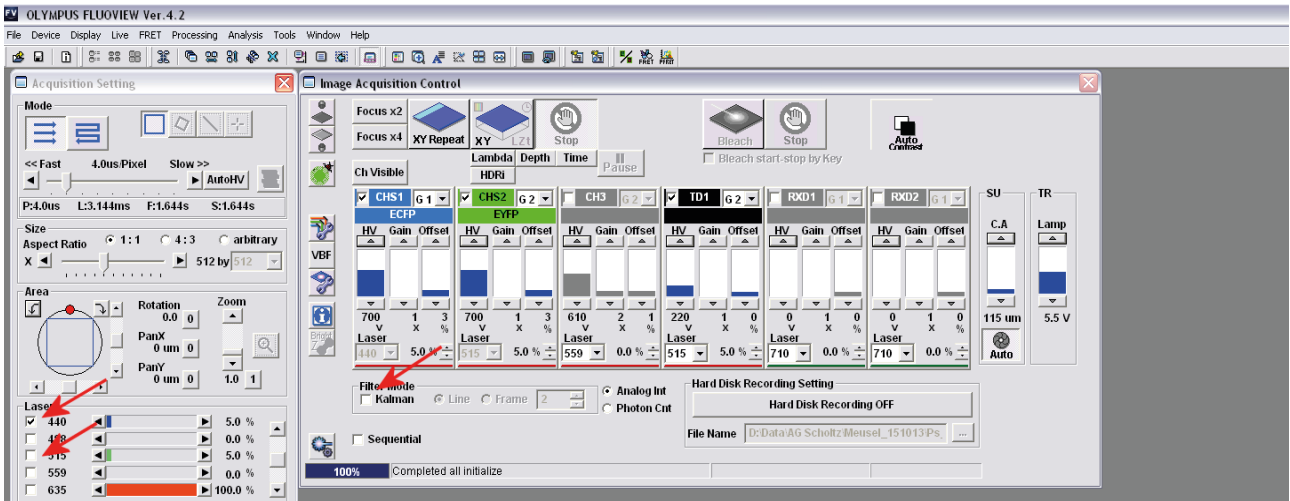


Figure A2 Settings of FV-1000 software for confocal imaging of CFP-YFP intensity FRET. Only 458 nm laser line is activated, CFP and YFP emission are detected in parallel.

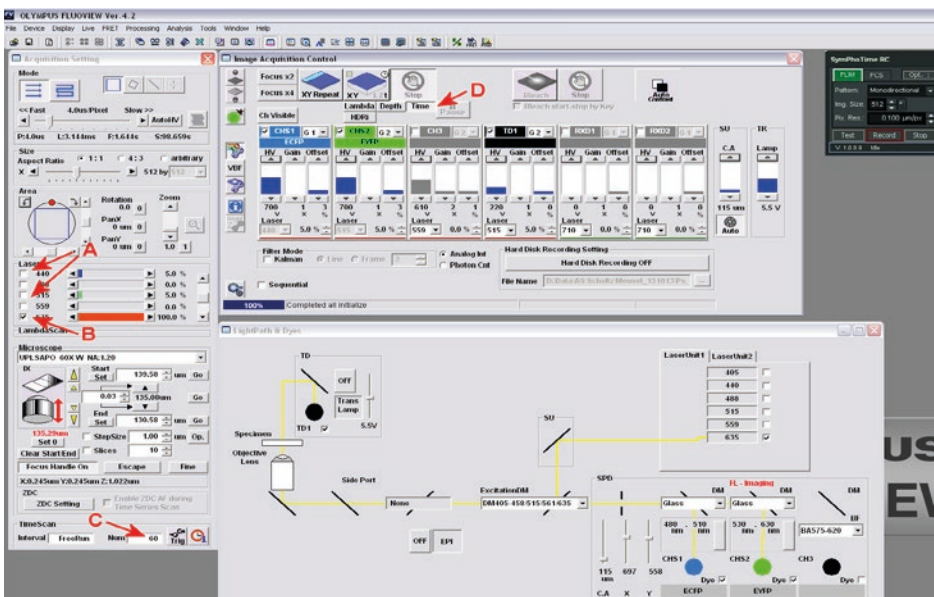


Figure A3 Settings of FV-1000 software for FLIM imaging of CFP fluorescence. Cw lasers lines are deactivated (A), pulsed diode laser on/off is controlled FV1000 software (B), TimeScan is set to free run, 60 frames and Time toggle is activated (C) and emission signal is routed to output port (D). SymphoTime on the FLIM computer can be controlled via SymphoTime_RC from the IMAGING computer.

used. The intensity has to be set to 100% enabling the on/off software control of the pulsed lasers, whereas power adjustment of the pulsed lasers has to be done manually at the Laser Combining Unit (LCU) or via the pulsed diode laser driver unit (PDL).

5. Acquisition of FLIM images

Adjust equal image size in *FluoView* and *SymPhoTime* software (e.g. 512 x 512 pixel). Reduce scan speed (pixel dwell time) to enable proper calculation of the average photon counts per pixel. Start scanning in the XY Repeat mode and activate "Test" with *SymPhoTime_RC*. Adjust laser power to a maximum <105 counts/second. When all adjustments are done, stop "Test" mode. You can set the filename, resolution (can be obtained from the "info" button of *FluoView*) and additional comments for the FLIM file using

SymPhoTime_RC.

For the acquisition of the FLIM image, activate the "Time" toggle button and set time settings to "Free run" and 60 scans, this will result in a FLIM acquisition time of about 90 seconds. Start FLIM recording with *SymPhoTime_RC* ("Record") and then start x-y-t acquisition in the *FluoView* software. After scanning has finished stop FLIM acquisition with *SymPhoTime_RC* ("Stop").

6. Measurement of the internal response function (IRF)

If there is no fluorophore solution with the spectral properties of CFP and a very short lifetime available, scattering of the excitation light is used to record the IRF. Put a drop of buffer on a cover slip and place a narrow-band laser-line filter in front of the detector. Set the scanning mode to point-scan

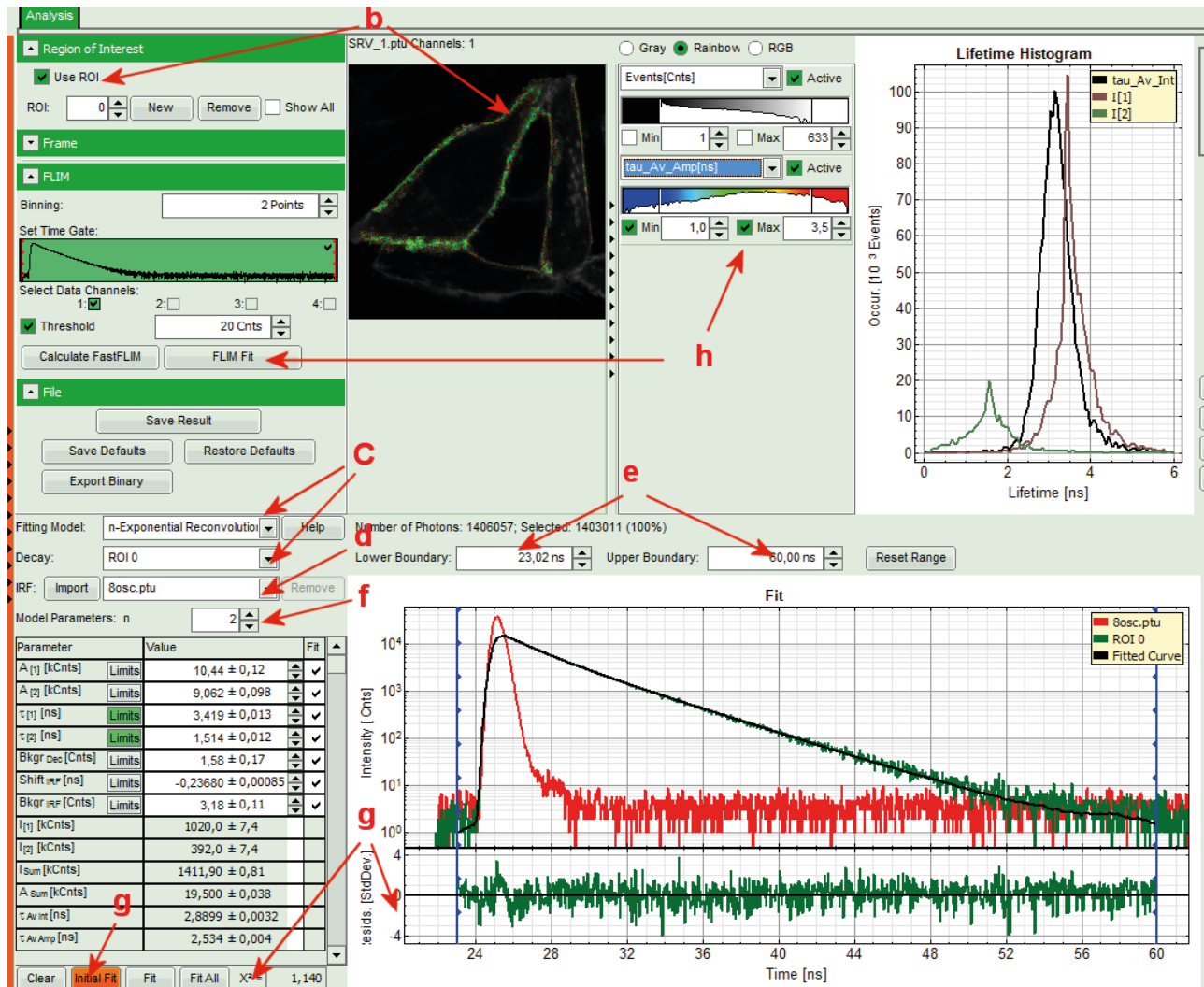


Figure A4 FLIM Image analysis with PicoQuant *SymPhoTime 64* software. (b) Selection of ROIs, (c) setting of fitting model and ROI, (d) loading of the IRF, (e) selection of range of channels, (f) selecting the number of exponentials for the fit, (g) fitting of the decay curve and analysis of the results and (h) finally lifetime fit for each individual point, generation of the lifetime image and the Lifetime histogram).

and the number of scans to 32.000. Start scanning in the XY Repeat mode and activate “Test” with *SymPhoTime_RC*. Attenuated the signal down to about 104 counts / second. Afterwards measure the decay curve as described for the FLIM images above for about 60 seconds.

7. Data Analysis

- a) In *SymPhoTime*, select the data set to be analyzed. With the latest version, *SymPhoTime 64*, choose “Analysis – Imaging – FLIM analysis”. The following steps are similar for the 32 and the 64 bit version of *SymPhoTime*. (see Figure A4)
- b) Activate “Use ROI” and mark one or more Regions of Interest (ROI) on the FLIM image using the selection tools (available by right-click on the image). We are interested in the interaction of TMD-HA-YFP with the raft-marker GPI-CFP, so we are selecting the plasma membrane of cells expressing both CFP and YFP (based on the confocal image data set 1)
- c) Set “Fitting Modell” to “n-Exponential Reconvolution” and select in “Decay” to the ROI you want to measure.
- d) Import the IRF measured and activate it (in the screenshot “8osc.ptu”) instead of the “Calculated IRF”
- e) Set the “Lower Boundary” and the “Upper Boundary” for the range of the fitted interval according to the measured decay curve.
- f) Set “Model Parameters: n” to the number of exponentials you want to fit your decay with. In our case, CFP is known to have a biexponential decay so we are starting with “2”.
- g) Do an “Initial Fit”, afterwards “Fit”. The fitted curve (black) should overlay well with the decay curve measured (green), quality of the fit is judged by the goodness of fit parameter χ^2 (should be close to 1) and the distribution of the residuals. The residuals representing the deviation of the fit from the measured decay curve should be small and randomly distributed. If the fit is not satisfying, especially if a tendency can be seen in the distribution of the residuals, an additional exponential should be added, all parameters have to be cleared and the fit has to be repeated.

The number parameters should be kept as low as possible and the parameters obtained have to be reasonable (for instance no lifetime below the resolution of the instrument, no negative amplitudes).

- h) When a satisfying fit has been obtained, the lifetime fit for each individual point of the selected ROI and the Lifetime histogram can be calculated with “FLIM Fit”. Calculation time can be reduced by Binning, but by doing so

resolution will be reduced. The color coding of can be adopted to optimize the contrast of the lifetime image.

(B) Video links for FLIM data acquisition

- Zeiss LSM 710 with a PicoQuant LSM Upgrade Kit (FLIM Demo)
- Nikon A1R with a PicoQuant LSM Upgrade Kit (FLIM and FCS Demo)
- Measuring a FLIM image with an LSM Upgrade Kit (Nikon A1)
- Recording a FLIM stack with an LSM Upgrade Kit on a Nikon A1
- Performing a FLIM-FRET Measurement with an LSM Upgrade Kit (Olympus FV 1200)
- Measure an Instrumental Response Function (IRF) with an LSM Upgrade Kit

(C) SPT64 links for FLIM data analysis

- SymPhoTime Lifetime Fitting
- Lifetime Fitting Using the FLIM Analysis
- FLIM ROI Fitting
- FLIM-FRET Calculation for Single
- Exponential Donors
- FLIM FRET Calculation for Multi Exponential Donors
- Pattern Matching
- Visualizing Dynamics with the Multi Frame FLIM Analysis
- Phasor Analysis

(D) Tipps/Tricks

- How to Measure the Instrument Response Function (IRF)
- How to Avoid the Pile-up Effect in FLIM Measurements

PicoQuant GmbH
Rudower Chaussee 29
12489 Berlin
Germany

Material can be downloaded from www.picoquant.com

© 2016 PicoQuant GmbH

All rights reserved. No parts of it may be reproduced, translated or transferred to third parties without written permission of PicoQuant GmbH.

www.picoquant.com